Dynamics of a glass-forming system: 11B NMR of B203

doi: 10.1063/1.469604

Dynamics of a glass-forming system: ^{11}B NMR of B_2O_3

Hideki Maekawa, Yousuke Inagaki, Shigezo Shimokawa,[a] and Toshio Yokokawa
Department of Chemistry, Faculty of Science, Hokkaido University, Sapporo 060, Japan

(Received 8 February 1995; accepted 28 March 1995)

The dynamics of the relaxation processes in a glass-forming system, B_2O_3, was investigated by means of ^{11}B nuclear magnetic resonance (NMR). Using a homemade high temperature NMR probe, we collected NMR data over a wide temperature range from room temperature to 1200 °C. The NMR data were interpreted in terms of a Fourier transform of the Kohlrausch decay function, $f(t)=\exp[-(t/\tau_c)^{-b}]$, where the parameter b varied from 0 to 1. The temperature dependence of τ_c and b in the decay function was estimated by using both the data from a ^{11}B NMR longitudinal relaxation and a line shape measurement at each temperature. Above 800 °C, the NMR data were well simulated by a single exponential decay of the function (i.e., $b=1$). Below 800 °C, stretched exponential was introduced to the simulation with the b parameters of 0.6 and 0.8. An Arrhenius plot of τ_c showed a bend at around 600 °C, which indicates the existence of two distinct reorientational processes crossing each other at that temperature. Below 600 °C, an almost linear dependence of the logarithm of τ_c vs the inverse of temperature with the activation energy of 40 kJ/mol was observed. This process persists below the glass transition temperature. Above 600 °C, the temperature dependence of τ_c became non-Arrhenius-like and was identical with that of the previous relaxation measurements. The isotropic chemical shift for the B_2O_3 melt suggests that the network structure constructed from the BO_3 triangle is preserved in the whole temperature range. © *1995 American Institute of Physics.*

I. INTRODUCTION

The dynamical processes in glass-forming liquids and their glass transitions have been investigated in a wide variety of substances using many different experimental techniques.[1–3] The complex dynamical behavior in the vicinity of the caloric glass transition temperature (T_g) has been phenomenologically described by distributions of the relaxation times. In particular, the Kohlrausch–Williams–Watts (KWW) distribution has been discussed in many recent theoretical treatments since it is a stretched exponential relaxation function and can be related to physical models of the glass transition.[4–6]

However, comparisons of these models with experimental data have the problem that most relaxation experiments provide rather indirect information about the molecular mechanisms involved. The advantage of nuclear magnetic resonance (NMR) methods is that they can probe the motion of well defined molecular vectors which can be directly related to the molecular motion itself.[6–10]

Recent measurements on relaxation processes reveal that the structural relaxation in glass-forming systems is characterized by two separate processes; the α and β processes.[6,9,11–15] The α process corresponds to those degrees of freedom which freeze out at T_g and are associated with the collective motion directly related to the liquid–glass transition, while the β process corresponds to those degrees of freedom which exist in both the liquid and glass and are associated with single particle motions.

Relaxation studies concerning the dynamical behavior of an organic glass-forming system in recent years have provided insight into the relationship between the structural relaxation and the dynamical behavior of molecular motion.[6–9,13,16] In contrast, the dynamics of an inorganic network glass-forming system, such as silicates and borates, have been poorly understood mainly due to experimental difficulties.[10,17–19]

Recently, our ^{11}B NMR longitudinal-relaxation study[20] demonstrated the temperature dependence of the reorientational correlation time (τ_c) of binary Na_2O–B_2O_3 melts. A crossover between two distinct orientational relaxation processes was observed well above the T_g. The non-Arrhenius character of the τ_c for both processes was discussed and analyzed on the basis of strong-fragile classifications.[21–26]

In the present study, we measured B_2O_3 which is one of the best studied examples among inorganic glass-forming materials. The spin-lattice relaxation and line shapes of ^{11}B in a B_2O_3 glass and melt were measured with ppm resolution over a wide temperature range from room temperature to 1200 °C. The temperature effect on the structure and dynamics of the supercooled liquid and the liquid state was studied.

B_2O_3 is a typical network glass-forming oxide whose caloric T_g and melting point are 260 and 577 °C, respectively. The structure of the B_2O_3 glass has been a much debated issue for many years.[27–32] It has been generally accepted that the B_2O_3 glass is constructed from a three-dimensional random network and its unit is a planar BO_3 triangle.[27–30] The manner in which the BO_3 triangles are connected seems to be still open to discussion. Spectroscopic observations of the B_2O_3 glass indicate the existence of the well defined boroxol ring (B_2O_6) molecular entity.[28,30] In contrast, molecular-dynamics simulation studies demonstrated that the B_2O_3 glass and melt structure do not necessarily contain the boroxol ring, and still adequately repro-

[a]NMR Laboratory, Faculty of Engineering, Hokkaido University, Sapporo 060, Japan.

duces the neutron and x-ray determined structure factors.[29] However, as a general view, it seems natural that vitreous B_2O_3 contains a large amount of boroxol rings. The ease of glass forming in this material seems to be correlated with this rigid geometry since the B_2O_3 crystal does not contain a boroxol ring.[33]

Viscosity measurements of B_2O_3 show a non-Arrhenius behavior in the region from 300 to 800 °C; above 800 °C a constant activation energy was found.[34–36] Sperry and Mackenzie[35] interpret this as evidence of a temperature-dependent structure, and deduce that molten B_2O_3 above 800 °C is composed of small unionized molecules. These molecules are presumably the same as those which exist in the vapor phase of B_2O_3.[37]

The non-Arrhenius behavior and the viscous relaxation in the B_2O_3 melt has also been investigated by several other groups.[38–40] The relaxation time spectra had been determined by the ultrasonic shear and longitudinal measurements and pressure jump relaxation measurements from 250 to 1000 °C.[39,40] These authors have demonstrated the existence of a wide distribution of activation energies in the α process of this melt. Both of a log-Gaussian distribution and a stretched exponential for the relaxation function were employed and the width of the distribution was quantified. Above 800 °C, in the region where the shear viscosity is Arrhenius, the shear relaxation process was characterized by a single relaxation time, whereas below 800 °C, an increasingly broad distribution of correlation time for the α relaxation process is suggested.

In a previous work concerning the ^{11}B NMR on B_2O_3 glass and melt by Rubinstein,[41,42] NMR relaxation data were analyzed based on the classical treatment given by Bloembergen, Purcell, and Pound (BPP).[43] The ^{11}B spin-lattice relaxation time of B_2O_3 was compared with that of the calculated one by deducing the ultrasonic attenuation measurements assuming a log-Gaussian distribution for the correlation times.[39] The author concluded that the high temperature nuclear relaxation is well understood in terms of the dynamics of the melt, corresponding to the α process monitored over the whole regime of the liquid state by NMR relaxation measurements.[42] In his analysis, the decay of the magnetization had been assumed to be a single exponential. However, the relaxation decay of the nucleus with the spin numbers of I is known to have a sum of $I+1/2$ exponential decays.[44–47] The BPP treatment of the relaxation data seem to lead to an extreme temperature dependence on τ_c in contrast with the present study. Here, the NMR relaxation data have been treated under still more accurate theoretical treatment rather than BPP, as will be shown later.

II. EXPERIMENT

NMR measurements were carried out on a Bruker MSL-200 spectrometer with a wide bore (150 mm) magnet operated at 64.19 MHz for ^{11}B. The high temperature NMR probe[20,48] specially reconstructed for this experiment was made of a platinum electric heater nonmagnetically wound and an outer water jacket. The detachable detection coil was made of platinum wire solenoidally turned six times.

Spin-lattice relaxation time measurements were performed using the inversion-recovery sequence (180°-delay-90°). The saturation-recovery sequence (a train of 90° pulses-delay-90°) was also employed to obtain some of the experimental points. However, both of them gave identical results within experimental error.

A 90° pulse length for the excitation of the magnetization was 4 μs from room temperature to 400 °C. However, it took more time as the temperature was increased to 1200 °C (a 90° pulse width was 12 μs at 1000 °C), because the quality factor of the detection coil decreased with temperature.

The reagent grade anhydrous B_2O_3 was melted in a platinum crucible at 1200 °C for 5 h, quenched to glass, and put into an alumina sample holder for the measurements.

In the present investigation, the longitudinal relaxation and line shapes were analyzed in terms of the theoretical formula given by Hubbard[44] and Werbelow[46] which had successfully explained our previous longitudinal-relaxation data.[20]

For the quadrupolar nucleus, an interaction between the electric field gradient at the nucleus (eq) and the nuclear quadrupole moment (eQ) produces an effective relaxation of the magnetization, if there is no other effective relaxation mechanism. For the particular case of ^{11}B ($I=3/2$), the relaxation behavior of the longitudinal magnetization is given by the following expression:[44]

$$\langle S_z\rangle-\langle S_z\rangle^T=-2\langle S_z\rangle^T[(4/5)\exp(-a_1t)+(1/5)\exp(-a_2t)], \tag{1}$$

where

$$a_1=2CJ_2,\ a_2=2CJ_1,\ C=(1/20)\cdot(e^2qQ/h)^2, \tag{2}$$

and

$$J_n=\mathrm{Re}\int_0^\infty\langle Y_2^k[\Omega(t)]Y_2^k[\Omega(0)]\rangle\exp(-in\omega t)dt, \tag{3}$$

where ω is the Larmor frequency expressed in radian, e^2qQ/h is the effective quadrupole-coupling constant, and J_n is a spectral density function of the molecular motion. $\langle S_z\rangle$ and $\langle S_z\rangle^T$ represent the longitudinal magnetization and its equilibrium value, respectively.

The transverse relaxation following the $\pi/2$ pulse is given by[46,47]

$$\langle S_x\rangle-i\langle S_y\rangle^T=\langle S_z\rangle^T i\ \exp[-i\omega(t-t_0)]\times[(3/5)\exp(-b_1t)+(2/5)\exp(-b_2t)], \tag{4}$$

where

$$b_1=C(J_0+J_1+iQ_1),\quad b_2=C(J_1+J_2-iQ_1+iQ_2). \tag{5}$$

The imaginary components of the spectral density are

$$Q_n=\mathrm{Im}\int_0^\infty\langle Y_2^k[\Omega(t)]Y_2^k[\Omega(0)]\rangle\exp(-in\omega t)dt, \tag{6}$$

which include hyperfine second-order dynamic quadrupolar shifts which cause a displacement of the satellite pairs and the central line relative to each other.

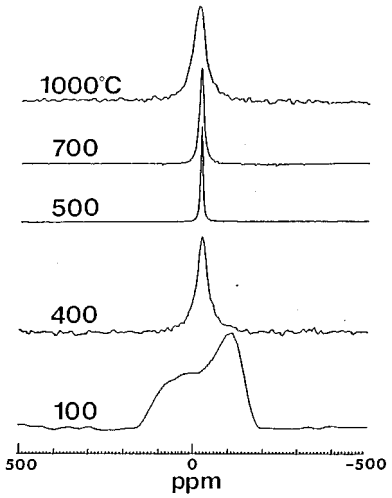

FIG. 1. Temperature variation of ^{11}B NMR spectra of B_2O_3.

In the present investigation, the correlation function of the spectral density is assumed to decay with a KWW function,

$$\langle Y_2^k[\Omega(t)]Y_2^k[\Omega(0)]\rangle = \exp[-(t/\tau_c)^{-b}], \tag{7}$$

where τ_c is the representative correlation time in the distribution of the stretched exponential scheme and the parameter b ranging from 0 to 1.

III. RESULTS

Figure 1 shows the temperature variation of the ^{11}B NMR spectra for the B_2O_3 glass and melt. The room temperature spectrum is characteristic of a rigid-lattice second-order quadrupolar line shape. A line shape simulation of the spectrum gives a static effective quadrupolar coupling constant (e^2qQ/h) of 2.6 ± 0.1 MHz which is in accordance with the previous studies.[27]

The ^{11}B NMR spectra for the B_2O_3 glass show little change before the T_g was reached. Above T_g, where B_2O_3 becomes a supercooled liquid, the linewidth steadily decreased until 550 °C. The full-width at half-maximum (FWHM) at 550 °C was 480 Hz (7.5 ppm). The FWHM then increased with increasing temperature. This anomalous temperature behavior of the FWHM is characteristic of the multiexponential quadrupolar relaxation when the correlation time is close to the inverse of the Larmor frequency which can be simulated by using Eq. (4).[46,47]

Both the longitudinal relaxation and the spectra have been simulated using Eqs. (1) and (4), respectively. Two parameters involved in this simulation, the stretching parameter b and the correlation time τ_c, have been adjusted so as to reproduce both the magnetization decay, which was fit using Eq. (1), and the line shape at this temperature. The line shape was compared with the calculated spectrum which is obtained by Fourier transforming the transverse-relaxation function, $\langle S_x\rangle - i\langle S_y\rangle$, in Eq. (4).

Figure 2 represents an example of the b value dependence of the fitting. On the left-hand side of the figure, the time evolution of the normalized longitudinal magnetization,

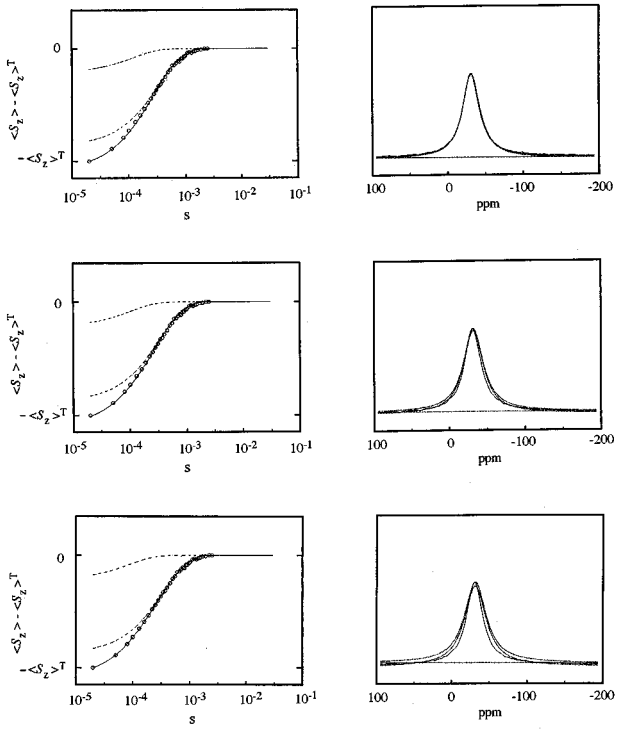

FIG. 2. Fitting of ^{11}B NMR longitudinal relaxation decay and spectrum for B_2O_3 melt at 763 °C showing the dependence on the b value. (Left) Normalized relaxation decay of the longitudinal magnetization after the final 90° pulse. Open circles are the experimental points. Solid lines are the simulation with Eq. (1), while the broken lines show the two components involved in the equation. (Right) Solid lines are the experimental spectrum. Dotted lines are the simulation showing each of the components. (Top) $\log(\tau_c) = -7.40$ and $b = 0.6$; (middle) $\log(\tau_c) = -7.65$ and $b = 0.8$; (bottom) $\log(\tau_c) = -7.82$ and $b = 1.0$.

$\langle S_z\rangle - \langle S_z\rangle^T$, of the ^{11}B nucleus in B_2O_3 melt at 763 °C, obtained by the saturation-recovery experiment, are shown. The solid lines in the figure are the best fit using the theoretical function of Eq. (1) with $b = 0.6$, 0.8, and 1.0, from top to bottom. The smaller b value gave the greater $\log(\tau_c)$ for the best fit. Each b value (0.6, 0.8, and 1.0) shows a satisfactory fitting for the longitudinal relaxation. However, as shown in the right-hand side in the figure, the calculated spectra for both $b = 0.8$ and $b = 1.0$ using the identical parameters obtained from the longitudinal fitting show systematic disagreement with the experimental spectra. The calculated spectra for $b = 0.8$ and 1.0 are slightly broader than the experimental spectrum, while the spectrum of $b = 0.6$ shows the best fit to the experimental spectrum. In this way, the temperature dependence of τ_c and b have been obtained from the ^{11}B data at each temperature.

In this simulation, the effective quadrupolar coupling constant was fixed at 2.67 MHz which is thought to be the most reliable value obtained by the ^{11}B NMR satellite transitions of the B_2O_3 glass.[49]

Above 800 °C, a reasonable fit was observed with a single exponential decay $(b = 1)$ of the spectral density function, thus the Debye behavior holds in this temperature range. On the other hand, below 800 °C, the stretched exponential was necessary to be introduced for the line shape simulation with the b parameter ranging from 0.6 to 0.8. The

TABLE I. The stretching parameter b and the logarithm of the correlation time $\log(\tau_c)$ obtained from ^{11}B NMR data for B_2O_3.

Temperature (°C)	$\log(\tau_c)$	b
300	−4.478	0.6
350	−4.966	0.6
400	−5.388	0.6
490	−5.940	0.6
500	−6.083	0.6
550	−6.35	0.6
600	−6.50	0.6
612	−6.58	0.6
650	−6.85	0.6
682	−7.02	0.6
716	−7.20	0.6
763	−7.40	0.6
800	−7.52	0.8
870	−7.79	1.0
920	−7.95	1.0
965	−8.07	1.0
1000	−8.14	1.0

final values for both b and τ_c obtained from the simulation are listed in Table I, and the temperature dependence of τ_c is shown in Fig. 3. α-Structural relaxation times obtained from the ultrasonic relaxation[39] and share viscosity measurements[38] are also cited in the figure. The shear relaxation time of the viscosity was calculated using the Maxwell equation

$$\eta_s = \tau_s G_\infty , \tag{8}$$

with $G_\infty = 10^{-10.8}$ which had been measured from the ultrasonic relaxation.[39]

In Fig. 4 are shown the comparison between the experimental and the calculated spectra. Agreement between each spectrum is quantitative.

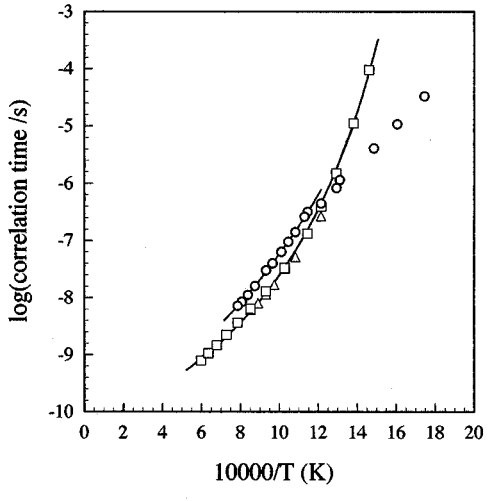

FIG. 3. Experimental and simulated spectra of ^{11}B NMR of B_2O_3. (Left) Experimental spectra at (a) 965 °C; (b) 870 °C; (c) 763 °C; (d) 716 °C; (e) 682 °C; (f) 612 °C; and (g) 550 °C. (Right) Simulated spectra with (h) $\log(\tau_c) = -8.07$ and $b = 1.0$; (i) $\log(\tau_c) = -7.79$ and $b = 1.0$; (j) $\log(\tau_c) = -7.40$ and $b = 0.6$; (k) $\log(\tau_c) = -7.20$ and $b = 0.6$; (l) $\log(\tau_c) = -7.02$ and $b = 0.6$; (m) $\log(\tau_c) = -6.58$ and $b = 0.6$; and (n) $\log(\tau_c) = -6.35$ and $b = 0.6$.

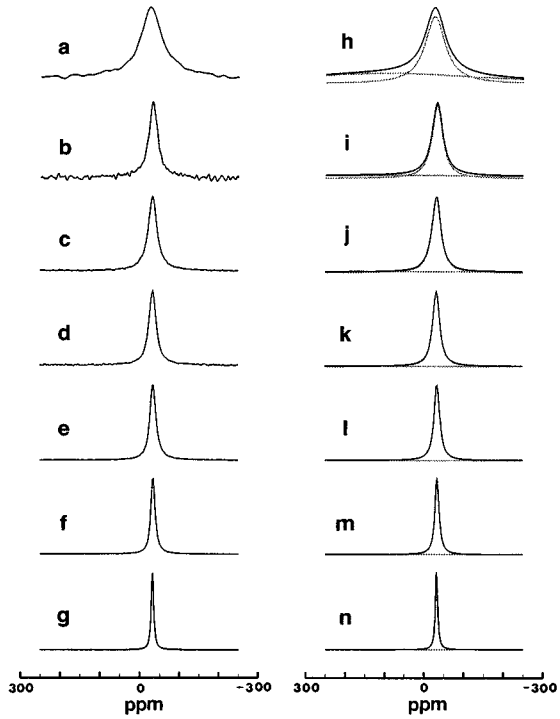

FIG. 4. Temperature dependence of the correlation times of the B_2O_3 melt. (○), reorientational correlation time of BO_3 triangles determined from the present ^{11}B NMR quadrupolar relaxation measurements. (△), α-structural relaxation times obtained from the ultrasonic relaxation measurements (Ref. 39). (□), α-structural relaxation times obtained from the share viscosity measurements (Ref. 38). The shear relaxation time of viscosity was calculated from the Maxwell equation [Eq. (7)] with $G_\infty = 10^{-10.8}$ (Ref. 39). Solid lines represent the result of VTF fits (see the text).

It should be noted that the isotropic chemical shift values could not directly obtained from the peak positions of raw spectra, because the peak positions of the ^{11}B NMR spectra are affected by the quadrupolar interaction, in which the imaginary component of Q_n in Eq. (5) is responsible.[46] Instead, the isotropic chemical shifts can be estimated from the experimental spectra used to correct the dynamic frequency shifts of Eq. (4) using parameters obtained from the line shape simulations. The estimated isotropic chemical shifts of ^{11}B for the B_2O_3 melt are shown in Fig. 5. They are located in the range for that of the BO_3 structural units.[31]

IV. DISCUSSION

A. The temperature dependence of τ_c

The temperature dependence of τ_c shows a bend at a temperature where the value is on the order of 10^{-6} s. In the high temperature region, the temperature dependence of τ_c is in agreement with that of correlation times derived from other structural relaxation measurements, whereas in the lower temperature region, the temperature dependence of τ_c largely deviates from that of other methods. Because of the distinct temperature dependence of both regions, it is naturally concluded that the presence of two dynamical processes are responsible for the ^{11}B relaxation. In the present investi-

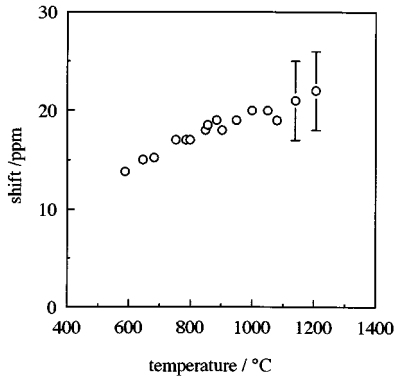

FIG. 5. Temperature dependence of ^{11}B chemical shift of the B_2O_3 melt obtained from the line shape simulation using Eq. (4).

gation, because the condition $\omega\tau_c > 1$ is fulfilled in the whole temperature range, the longitudinal relaxation is dominated by the higher frequency motion within the Larmor precession frequency.[44–47] Therefore, the bend in Fig. 3 corresponds to the ''crossover'' from one dynamical process to the other which has the shorter correlation time in the temperature ranges above and below the crossover temperature.

Above the crossover temperature, τ_c are characteristic of the α process in the glass-forming systems, because the τ_c obtained from the present NMR measurement shows a very similar temperature dependence with that of viscosity and ultrasonic longitudinal relaxation measurements. However, it was smaller by a factor of 2 than those from other measurements. This small disagreement may result from the difference in the mechanism which is responsible for each relaxation process.

The NMR quadrupole relaxation proceeds by a fluctuation in the electric field gradients around the nucleus under investigation. For the B_2O_3 melt, the orientational fluctuation of the BO_3 triangle is expected to play a major role in the relaxation of the magnetization. Thus, the NMR relaxation includes the contribution from the orientational processes in addition to the translational diffusion processes. This may introduce the discrepancy for the correlation times between the structural relaxation times obtained from the ultrasonic elastic and viscosity measurements and the present NMR measurements.

In Fig. 3, the temperature dependence of τ_c shows almost a linear dependence vs the inverse temperature below 600 °C with a relatively lower activation energy. This is in contrast with the previous results given by Rubinstein,[42] where the correlation times were more temperature dependent. The low activation energy for this motion (40 kJ/mol) suggests this is not directly related to the structural relaxation processes. Translational and/or rotational diffusion presumes simultaneous breaking of the strong B–O bonds since the B_2O_3 melt is constructed from a three-dimensional network. The restricted rotation (rotational vibration) of the structural units around its equilibrium positions will probably be responsible for this process.

On the other hand, above 600 °C, τ_c becomes strongly temperature dependent and non-Arrhenius. The temperature dependence of the correlation times of the glass-forming systems corresponding to the α-structural relaxation is usually non-Arrhenius over a certain temperature range above the T_g. The degree of departure from Arrhenius behavior leads to the strong- and fragile-liquid classification introduced by Angell for which theoretical interpretations are currently being sought.[21–26] The correlation time of strong liquids is usually well approximated by the Arrhenius temperature dependence, while that of fragile liquids is better approximated by the Vogel–Tamman–Fulcher (VTF) equation

$$\log \tau_c = A + [DT_0/(T - T_0)],$$

where D is the dimensionless parameter which characterizes the curvature of the Arrhenius plot, and the ''fragility'' of the liquid is denoted by parameter D.[21] The parameters used to fit the VTF equation are given in Table II. The VTF parameters of the α-structural relaxation (viscosity)[34] are also cited in the table.

TABLE II. Results of the VTF fits for ^{11}B NMR correlation times (present results) and of the viscosity data (Ref. 38).

	A	D_0	T_0(K)
Viscosity	−10.28	3.34	445
NMR	−10.33	5.96	341

A very similar character for both of the structural and NMR orientational correlation times is obtained. However, the D value for the NMR orientational relaxation is smaller than that of the structural relaxation of the viscosity. This indicates that the degradation of the intermediate-range order preferentially releases the orientational degrees of freedom to a larger extent than do the translational degrees of freedom.

B. Chemical shift

The relationships between the ^{11}B chemical shift and the coordination environment around the boron nucleus have been studied on some materials.[31] The chemical shift of BO_3 is located in the range of 12.7–19.0 ppm, while that of BO_4 is in the range from −3.3–2.0 ppm referred from $BF_3 \cdot Et_2O$. The chemical shift for the B_2O_3 melt in Fig. 5, estimated from the line shape simulation, was roughly in the range for BO_3 over the whole temperature range studied in the present investigation. This is in accordance with the first RDF peaks in the neutron scattering measurements, which are nearly independent of temperature.[30] The progressive shift with temperature towards a positive direction is likely caused by the gradual change in the connectivity of the BO_3 units. A progressive fragmentation of the boroxol ring into unionized molecules had been suggested above 800 °C. Both Raman and neutron scattering studies suggested the molecule to be of a bipyramidal structure which is present in the vapor phase of B_2O_3. However, such a drastic structural change in the structure is not likely to produce the gentle temperature dependence of the chemical shift observed in the present investigation.

V. CONCLUSIONS

The high temperature NMR line shape and relaxation time measurements were made on ^{11}B in B_2O_3 melts. Longitudinal relaxation times and line shapes were well analyzed by multiexponential relaxation and dynamic frequency shifts with a Kholrausch decay for the spectral density function. Below 600 °C, the temperature dependence of the reorientational correlation time showed characteristics of a β-relaxation process which is attributable to the restricted rotation of the BO_3 triangles around its equilibrium position. On the other hand, above 600 °C, the correlation times showed a strong temperature dependence. Isotropic chemical shifts and reorientational correlation times of the BO_3 triangle were obtained. Isotropic chemical shifts gradually moved in a positive direction with increasing temperature. Above 800 °C, a single correlation time was enough to describe the spectrum profile as well as the relaxation.

ACKNOWLEDGMENTS

This research has been partly supported by a Grant-in-Aid for Scientific Research from the Ministry of Education, Science, and Culture of the Japanese Government (No. 04554025). H. M. appreciates the support of the Corning Research Grant.

[1] W. Götze, in *Liquids, Freezing and Glass Transition*, edited by J. P. Hansen, D. Levesque, and J. Zinn-Justin (Elsevier, Amsterdam, 1989), pp. 292–498.
[2] C. A. Angell, Chem. Rev. **90**, 523 (1990).
[3] G. H. Fredrickson, Annu. Rev. Phys. Chem. **39**, 149 (1988).
[4] R. Kohlraush, Pogg. Ann. Phys. **12**, 393 (1847).
[5] G. Williams and D. C. Watts, Trans. Faraday Soc. **66**, 80 (1970).
[6] Th. Dries, F. Fujara, M. Kiebel, E. Rössler, and H. Sillescu, J. Chem. Phys. **88**, 2139 (1988); **90**, 7613(E) (1989).
[7] E. Rössler and H. Sillescu, Chem. Phys. Lett. **112**, 94 (1984).
[8] S. Kaufmann, S. Wefing, D. Schaefer, and H. W. Spiess, J. Chem. Phys. **93**, 197 (1990).
[9] E. Rössler, J. Chem. Phys. **92**, 3725 (1990).
[10] I. Farnan and J. F. Stebbins, Science **265**, 1206 (1994).
[11] G. P. Johari and M. Goldstein, J. Chem. Phys. **53**, 2372 (1970).
[12] B. Bagchi, A. Chandra, and S. A. Rice, J. Chem. Phys. **93**, 8991 (1990).
[13] E. Rössler, Phys. Rev. Lett. **65**, 1595 (1990).
[14] D. Kivelson and S. A. Kivelson, J. Chem. Phys. **90**, 4464 (1989); **92**, 819(E) (1990).
[15] D. Kivelson, J. Phys. Chem. **95**, 709 (1991).
[16] E. Rössler, A. P. Sokolov, A. Kisliuk, and D. Quitmann, Phys. Rev. B **49**, 14 967 (1994).
[17] S. Ganguly, R. Parthasarathy, K. J. Rao, and C. N. R. Rao, J. Chem. Soc. Faraday Trans. 2 **80**, 1395 (1984).
[18] A. P. Sokolov, A. Kisliuk, and D. Quitmann, Phys. Rev. B **48**, 7692 (1993).
[19] A. P. Sokolov, E. Rössler, A. Kisliuk, and D. Quitmann, Phys. Rev. Lett. **71**, 2062 (1993).
[20] Y. Inagaki, H. Maekawa, S. Shimokawa, and T. Yokokawa, Phys. Rev. B **47**, 674 (1993).
[21] C. A. Angell, J. Non-Cryst. Solids **102**, 205 (1988).
[22] M. Tatsumisago, B. L. Halfpap, J. L. Green, S. M. Lindsay, and C. A. Angell, Phys. Rev. Lett. **64**, 1549 (1990).
[23] H. He and M. F. Thorpe, Phys. Rev. Lett. **54**, 2107 (1985).
[24] F. H. Stillinger, J. Chem. Phys. **88**, 7818 (1988).
[25] J. P. Sethna, J. D. Shore, and M. Huang, Phys. Rev. B **44**, 4943 (1991).
[26] R. Böhmer and C. A. Angell, Phys. Rev. B **45**, 10 091 (1992).
[27] A. H. Silver and P. J. Bray, J. Phys. Chem. **29**, 984 (1958).
[28] R. L. Mozzi and B. E. Warren, J. Appl. Crystallogr. **3**, 251 (1970).
[29] Q. Xu, K. Kawamura, and T. Yokokawa, J. Non-Cryst. Solids **104**, 261 (1988).
[30] M. Misawa, J. Non-Cryst. Solids **122**, 33 (1990).
[31] G. L. Turner, K. A. Smith, R. J. Kirkpatrick, and E. Oldfield, J. Magn. Reson. **67**, 544 (1986).
[32] A. K. Hassan, L. M. Torell, L. Bjesson, and H. Doweidar, Phys. Rev. B **45**, 12 797 (1992).
[33] S. L. Strong and R. Kaplow, Acta Crystallogr. Sect. B **24**, 1032 (1968); S. L. Strong, A. F. Wells, and R. Kaplow, *ibid*. **27**, 1662 (1971).
[34] P. B. Macedo and A. Napolitano, J. Chem. Phys. **49**, 1887 (1968).
[35] L. L. Sperry and J. D. Mackenzie, Phys. Chem. Glasses **9**, 91 (1968).
[36] J. Boow, Phys. Chem. Glasses **8**, 45 (1967).
[37] P. L. Hanst, V. H. Early, and W. Klemperer, J. Chem. Phys. **42**, 1097 (1965).
[38] P. Macedo and T. A. Litovitz, Phys. Chem. Glasses **6**, 69 (1965).
[39] J. Tauke, T. A. Litovitz, and P. B. Macedo, J. Am. Ceram. Soc. **51**, 158 (1968).
[40] J. A. Bucaro, H. D. Dardy, and R. D. Corsaro, J. Appl. Phys. **46**, 1975 (1975).
[41] M. Rubinstein and H. A. Resing, Phys. Rev. B **13**, 959 (1976).
[42] M. Rubinstein, Phys. Rev. B **14**, 2778 (1976).
[43] N. Bloembergen, E. M. Purcell, and R. V. Pound, Phys. Rev. **73**, 679 (1948).
[44] P. S. Hubbard, J. Chem. Phys. **53**, 985 (1970).
[45] A. G. Redfield, IBM J. January 19 (1957).
[46] L. Werbelow and G. Pouzard, J. Phys. Chem. **85**, 3887 (1981).
[47] G. Jaccard, S. Wimperis, and G. Bodenhausen, J. Chem. Phys. **85**, 6282 (1986).
[48] S. Shimokawa, H. Maekawa, E. Yamada, T. Maekawa, Y. Nakamura, and T. Yokokawa, Chem. Lett. **1990/4**, 617 (1990).
[49] P. W. France and M. Wadsworth, J. Magn. Reson. **49**, 48 (1982).